

Cite this: *Analyst*, 2011, **136**, 2464[www.rsc.org/analyst](http://www.rsc.org/analyst)

PAPER

# A long-lived luminescence and EPR bimodal lanthanide-based probe for free radicals†

Jinqing Hong, Yuanming Zhuang, Xiang Ji and Xiangqun Guo\*

Received 15th November 2010, Accepted 6th April 2011

DOI: 10.1039/c0an00914h

We developed a novel spin-labeled terbium complex Tb<sup>3+</sup>/cs124-DTPA-TEMPO (**1**) by covalently labeling a nitroxide radical on the terbium complex for monitoring free radicals of various areas. This lanthanide complex probe shows a high EPR signal which resulted from the nitroxide radical moiety, and is weakly luminescent which resulted from the intramolecular quenching effect of the nitroxide radical on sensitised terbium luminescence. The intensity of both the EPR and luminescence can be modulated by eliminating the paramagnetism of the nitroxide radical through recognition of a carbon-centered radical analyte and thus gives a quantification of the analyte. We have preliminarily applied this probe in the luminescent detection of model carbon-centered radicals and hydroxyl radicals ( $\cdot\text{OH}$ ). This probe is water-soluble and contains lanthanide-luminescence properties, favorable for the time-resolved luminescence technique. The investigation of the intramolecular quenching process has showed that the labeled nitroxide radical quenches multiple excited states of the terbium complex, resulting in highly efficient quenching of terbium luminescence. This probe is the first example of intramolecular modulation of lanthanide luminescence by a nitroxide radical.

## Introduction

The luminescent lanthanide complexes have been increasingly employed in the detection of biologically important analytes due to their long emission lifetimes, which enable the removal of light scattering and short-lived background autofluorescence.<sup>1–4</sup> Because of the low absorption coefficient of lanthanide ions, their excitation is usually performed through light-harvesting sensitizers or antennas. In a lanthanide complex, the sensitizer, usually aromatic ring or  $\beta$ -diketone incorporated in the ligand, absorbs a photon and transits to its singlet excited state, followed by intersystem crossing (ISC) to its triplet excited state. Then the energy is transferred to the lanthanide ion, resulting in lanthanide emission.<sup>2,4</sup> Whichever excited state, the singlet or triplet excited state of the sensitizer, or the excited state of lanthanide ions, is quenched, it can lead to the quenching of the final lanthanide luminescence intensity. A variety of responsive lanthanide-based probes have been developed based on the modulation of the excited-state population. Nagano *et al.* have

reported a systematic study for rational design of lanthanide-based probes, which consist of three moieties: a lanthanide chelate, a sensitizer and a luminescence off/on switch, based on intramolecular photoinduced electron transfer (PeT) modulation.<sup>5</sup> When the HOMO level of the switch moiety is high enough to induce PeT to the sensitizer, the singlet excited state of the sensitizer would be quenched, resulting in no lanthanide luminescence. Thus, a model PeT-based off/on luminescent lanthanide probe was synthesized for probing leucine aminopeptidase (LAP) based on the LAP-mediated reaction. Modulation based on triplet–triplet quenching has been reported in the lanthanide-based probe for singlet oxygen.<sup>6,7</sup> The triplet state of the terpyridine sensitizer moiety in the lanthanide-based probe was quenched by the anthracene moiety connected to the sensitizer, resulting in weak europium luminescence. On reacting with singlet oxygen, the anthracene moiety transformed to an endoperoxide and the triplet state quenching was blocked. The luminescence increase gave a quantitative detection of singlet oxygen. A ratiometric luminescence method for measuring uric acid in biological fluids based on lanthanide excited state quenching by electron transfer modulation has also been reported, and Tb complexes proved to be more sensitive to urate quenching than Eu analogues.<sup>8</sup> Due to the long lifetime of lanthanide luminescence, time resolved fluorescence resonance energy transfer (TR-FRET) biochemical assays have become widely used. Commercially available CisBio's HTRF technology,<sup>9</sup> relying on FRET with the lanthanide as energy donor and organic dye as acceptor, can eliminate false signal induced

*The Key Laboratory for Chemical Biology of Fujian Province, the Key Laboratory of Analytical Science and Department of Chemistry, College of Chemistry and Chemical Engineering, Xiamen University, Xiamen, China. E-mail: xqguo@xmu.edu.cn; Fax: +86 592 2188612*

† Electronic supplementary information (ESI) available: Detailed experimental section, HPLC chromatogram of product purification, the absorption spectra of **1** and **2**, the reaction of AIBN photolysis, and the EPR decrease of **1** trapping carbon-centered radicals. See DOI: 10.1039/c0an00914h

from direct excitation of the organic dye molecule. Johansson *et al.* reported a probe for DNA.<sup>10</sup> An oligonucleotide of known sequence was linked with Tb complex and quencher at each end respectively. The luminescence was modulated by spatially separating the Tb and quencher moieties due to hybridization or nuclease digestion. In addition, the design of the responsive lanthanide-based probe has also relied on changing the structure and optical property of the sensitizer,<sup>11–14</sup> and modulating the distance separating the sensitizer from the lanthanide ion.<sup>15–17</sup> To sum up, a rational design of lanthanide-based luminescence probes according to different modulating mechanisms opens ways to considerable development.

For modern biological analysis, molecular probes are required to access specific molecular events in the spatio-temporal domain, thus developing multi-modal probes has gained increasing interest during the last decade. Spin-labeling studies, based on electron paramagnetic resonance (EPR), provide a powerful tool for nanometre-scale distance determinations in biomolecules.<sup>18</sup> Spin-labeled fluorescent bimodal probes combine the virtues of both spin-labeling and fluorescent signaling, and open new windows to biological analysis.<sup>19</sup> A spin-labeled fluorescent probe consists of a fluorophore unit and a tethered stable nitroxide radical.<sup>20</sup> As a paramagnetic group, the nitroxide moiety quenches the excited state of the fluorophore efficiently,<sup>21–24</sup> keeping the probe's prefluorescent property. The fluorophore emission can be readily restored when the nitroxide moiety of a spin-labeled fluorescent probe is coupled with a carbon-centered radical (R) to eliminate its paramagnetic property. Hitherto most of the fluorophores involved are conventional organic fluorophores, and a number of organic fluorophore-nitroxide off/on probes have been designed for monitoring carbon-centered radical processes in polymer science,<sup>25–28</sup> biological systems<sup>29–32</sup> and environmental chemistry.<sup>33–35</sup> This method has also been used to detect hydroxyl radicals (OH), which reacts with dimethyl sulfoxide (DMSO) to produce a methyl radical (CH<sub>3</sub>) quantitatively.<sup>36–41</sup> A few papers have studied the effect of the nitroxide radical on lanthanide luminescence. An earlier study demonstrated that luminescence of the Tb<sup>3+</sup>/EDTA complex was quenched by the nitroxide radical 4-hydroxy-TEMPO (TEMPO = 2,2,6,6-tetramethylpiperidinyloxy, free radical).<sup>23</sup> It indicated that the quenching rate constant for the nitroxide radical in quenching the triplet state of terbium ion was 4 orders of magnitude smaller than those in quenching the singlet states of organic fluorophores. Rivera and Hudson have studied the quenching of Tb emission in the sensitised complex Tb<sup>3+</sup>/DTPA-cs124 by 4-hydroxy-TEMPO through an intermolecular collisional process, and observed a lifetime decrease of Tb luminescence simultaneously.<sup>42</sup> According to their observation, obvious quenching of Tb luminescence was achieved at a considerable high concentration of TEMPO (mM magnitude). This low quenching efficiency might have been attributed to an intermolecular mechanism.

Considering the modulating effect of the distance between the quencher and the luminophore on the luminescence of a lanthanide complex, we expected that the efficiency of intramolecular quenching would be much higher than that of intermolecular quenching. To develop a highly sensitive lanthanide-based luminescent probe, we designed and synthesized a spin-labeled lanthanide complex, Tb<sup>3+</sup>/cs124-DTPA-TEMPO (**1**), shown in

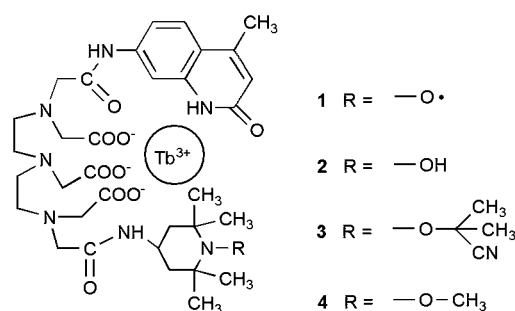


Chart 1

Chart 1, and explored its characteristics in terms of probing free radicals. In the structure of **1**, the DTPA structure provides a scaffold for high complexation strength with the Tb<sup>3+</sup> ion, and the organic chromophore cs124, covalently linked to DTPA, is one of the most efficient energy-transfer sensitizers yet synthesized for Tb<sup>3+</sup> and can induce Tb<sup>3+</sup> highly luminescent.<sup>43</sup> The paramagnetic TEMPO moiety is expected to quench Tb luminescence intramolecularly, acting as both EPR and luminescence switch. And the switch can be manipulated by trapping a carbon-centered radical, thus **1** can act as a bimodal free radical sensor. The results demonstrated that this lanthanide-based luminescence probe is weakly luminescent, due to the intramolecular quenching effect of the labeled nitroxide radical group. On trapping a carbon-centered free radical, the weakly luminescent probe readily transformed to a highly luminescent compound, synchronically with a disappearance of EPR signal. This probe is the first example of intramolecular modulation of lanthanide luminescence by a nitroxide radical.

## Experimental section

### Apparatus

The emission spectra were recorded on a RF-5301PC spectrofluorophotometer (Shimadzu). The excitation wavelength was 328 nm or 340 nm, and the intensities of cs124 and Tb luminescence were acquired at 367 nm and 546 nm, respectively. EPR measurements were performed using a Bruker EMX X-Band EPR spectrometer. All microwave parameters were kept constant, approximately 9.8 GHz microwave frequency, 20 mW microwave power, 10 dB attenuator, 100 kHz modulation frequency, 1.0 G modulation amplitude and 20 ms time constant. All measurements were carried out in 10 mM Tris-HCl buffer solution at pH 7.4 unless otherwise specified.

### Synthesis of chelator cs124-DTPA-TEMPO

1 equiv of DTPA (diethylenetriamene-pentaacetic) dianhydride, 0.8 equiv of 4-amino-TEMPO and 1.4 equiv of cs124 (7-amino-4-methyl-2(1H)-quinolinone) were dissolved in a mixture of anhydrous dimethyl sulfoxide (DMSO) and triethylamine. The reaction mixture was stirred at room temperature for 4 h. The reaction was quenched by addition of water, and continued to be stirred for 2 h. The product cs124-DTPA-TEMPO was separated from byproducts by HPLC reverse-phase, which was performed on a LC-10Avp HPLC system (Shimadzu) with a Diamonsil C18

column (250 × 4.6 mm, 5 μ, Dikma). The mobile phase was 40% methanol/TEAA (TEAA = 0.1 M triethylammonium acetate buffer, pH 6.0). The eluted fractions were monitored with a UV detector at a wavelength of 328 nm. The product peak was identified and collected (Fig. S1†). The yield was about 20%, as judged from the HPLC profile. HR-MS (ESI): calculated for C<sub>33</sub>H<sub>49</sub>N<sub>7</sub>O<sub>10</sub> (MH<sup>+</sup>) 703.3535, observed 703.3525. For NMR measurement, the nitroxide radical of the product was reduced to hydroxylamine by ascorbate, and then purified by HPLC. <sup>1</sup>H NMR (NaOD/D<sub>2</sub>O, Bruker Avance II 400 MHz): δ (ppm) 7.74 (1H, d), 7.58 (1H, s), 7.19 (1H, d), 6.44 (1H, s), 4.43 (2H, s), 3.88 (4H, s), 3.70 (4H, s), 3.57 (4H, t), 3.49 (4H, t), 2.72 (3H, s), 1.93 (4H, d), 1.01 (6H, s), 0.98 (6H, s). There was probably one unresolved H in 3.6–4.3.

### Preparation of Tb<sup>3+</sup>/cs124-DTPA-TEMPO (1)

**1** was formed by adding an excess of TbCl<sub>3</sub> to the cs124-DTPA-TEMPO solution and purified by the same reverse-phase HPLC system as mentioned above, and confirmed by HR-MS (ESI): calculated for C<sub>33</sub>H<sub>46</sub>N<sub>7</sub>O<sub>10</sub>Tb (MH<sup>+</sup>) 859.2554, observed 859.2545. **1** was then dissolved in 10 mM Tris-HCl buffer at pH 7.4 for use.

### Determination of quantum yields of Tb luminescence

The Tb quantum yields of the **1** and **2** were measured in diluted solutions with absorbance < 0.05 in 10 mm cuvette by the comparative method, according to the following equation:

$$\Phi_x = \Phi_{\text{std}} \frac{I_x}{I_{\text{std}}} \frac{A_{\text{std}}}{A_x} \frac{n_x^2}{n_{\text{std}}^2}$$

where  $\Phi$  is the quantum yield,  $I$  is the integrated area of the corrected emission spectrum,  $A$  is absorbance at the excitation wavelength,  $n$  is the refractive index, and the subscripts  $x$  and  $\text{std}$  refer to Tb complex and the standard, respectively. Quinine bisulfate in 1 N sulfuric acid in aqueous solution was employed as a standard ( $\Phi_{\text{std}} = 0.546$ ).<sup>44</sup> The absorption and excitation wavelength of 340 nm was selected, and ascorbate in the solution of **2** did not absorb light at this wavelength. The corrected emission spectra were recorded on a FluoroMax-4 spectrofluorometer (HORIBA Jobin Yvon).

### Determination of lifetimes

Decays of Tb luminescence were recorded on a LS 55 fluorescence spectrophotometer (Perkin Elmer) equipped with a pulsed xenon lamp (less than 10 microseconds duration). The excitation wavelength was 340 nm, and the intensities of Tb luminescence were acquired at 546 nm. Its FL WinLab software was used for exponential fitting.

Decays of cs124 luminescence were recorded on a FluoroMax-4 spectrofluorometer (HORIBA Jobin Yvon), using the TCSPC (time correlated single photon counting) method. The excitation source was a pulsed 281 nm NanoLED, and the photons were collected at 367 nm. The deconvolution and exponential fitting were performed using the DAS6 software (HORIBA Jobin Yvon); the average lifetimes were calculated using the equation:

$$\bar{\tau} = \frac{\sum_{i=1}^n \alpha_i \tau_i^2}{\sum_{i=1}^n \alpha_i \tau_i}$$

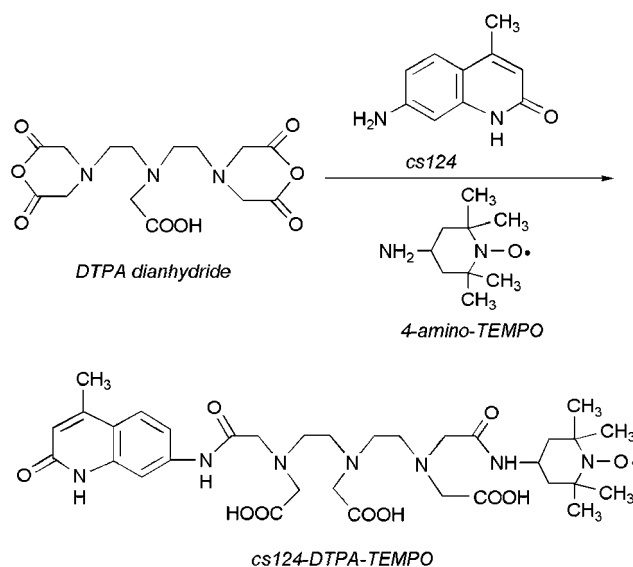
where  $\tau_i$  is the fluorescence lifetime and  $\alpha_i$  is the pre-exponential factor.

## Results and discussion

### Synthesis and property of 1

The synthesis of the spin-labeled lanthanide complex **1** was carried out by a method modified from the literature on lanthanide complexes of DTPA derivatives.<sup>45</sup> In the synthesis of the chelator cs124-DTPA-TEMPO (Scheme 1), the two anhydride groups of DTPA dianhydride reacted with amino groups of cs124 and 4-amino-TEMPO at room temperature. The product cs124-DTPA-TEMPO was well-separated from byproducts by reverse-phase HPLC (Fig. S1†), with starting material and byproducts appearing at different retention times and being identified respectively. The synthesis of the chelator is straightforward, and the yield is satisfactory. The chelator bound strongly with Tb<sup>3+</sup> ion in aqueous solution to form the spin-labeled lanthanide complex, Tb<sup>3+</sup>/cs124-DTPA-TEMPO (**1**). This preparation was confirmed by <sup>1</sup>H NMR and high resolution mass spectrometry. The TEMPO moiety of this complex gave an intense three-line EPR spectrum centered at  $g = 2.006$  (black line in Fig. 1c), characteristic of nitroxide radical.

To study the quenching effect of the tethered nitroxide radical on the Tb luminescence, the nitroxide radical of **1** was reduced to hydroxylamine derivative (**2** in Chart 1) by ascorbate,<sup>46</sup> changing the paramagnetic group to a diamagnetic one. A 30-fold increase in Tb luminescence (the Tb quantum yields were 0.5% and 15% for **1** and **2** respectively), concomitant with a decrease in EPR signal of TEMPO moiety, was observed in the presence of an excess of ascorbate (Fig. 1). The correlation between the elimination of the paramagnetism of nitroxide radical and the



**Scheme 1** The synthesis of chelator cs124-DTPA-TEMPO.

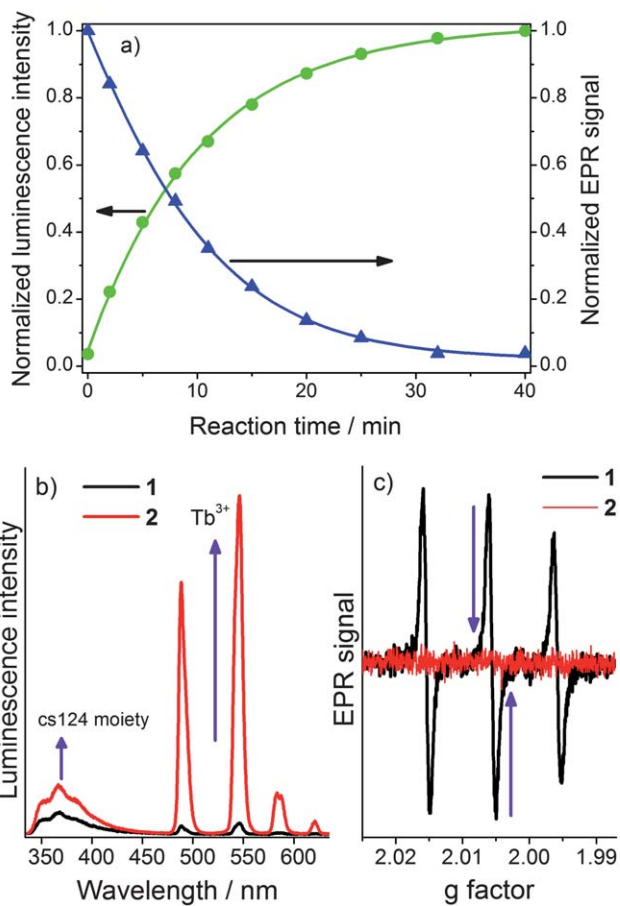


**Fig. 1** (a) Time-dependent TEMPO EPR signal (blue,  $g = 2.006$ ) and Tb luminescence (green,  $\lambda_{\text{ex}} = 328 \text{ nm}$ ,  $\lambda_{\text{em}} = 546 \text{ nm}$ ) following addition of  $100 \mu\text{M}$  ascorbate to a solution of  $10 \mu\text{M}$  of **1** in  $10 \text{ mM}$  Tris-HCl buffer at pH 7.4. (b) Comparison of luminescence spectra ( $\lambda_{\text{ex}} = 328 \text{ nm}$ ) and (c) EPR spectra of **1** and **2**.

restoration of Tb luminescence gives a sound evidence that nitroxide radical intramolecularly quenches the luminescence of Tb complex efficiently. The efficiency of intramolecular quenching of Tb luminescence by TEMPO is much larger than that of intermolecular quenching. And the quenching can be inhibited by eliminating the paramagnetism of nitroxide moiety. Thus the valuable EPR spectroscopic and preluminescent properties of **1** make it a potential bimodal probe for bioassays.

### Trapping of carbon-centered radicals

The nitroxide radical of **1** can trap carbon-centered radicals to produce a diamagnetic alkoxyamine, and lose its ability to quench the luminescence of Tb complex. Therefore, this novel spin-labeled lanthanide complex can act as an EPR and luminescence probe for carbon-centered radicals, allowing the use of time-resolved luminescence measurement. For this purpose, the response of **1** to carbon-centered radicals was explored. A model carbon-centered radical (R) was generated photolytically from a carbon-centered radical precursor AIBN (Scheme S1†). AIBN can be used as a photochemical or thermal radical source and has proved useful as a radical source with other prefluorescent probes.<sup>47</sup> Under an excess of AIBN, the increase of Tb

luminescence intensity showed a linear dependency on irradiation time at first, attributable to the production of complex **3** (Chart 1); and then leveled off after a period of time, attributable to running out of nitroxide radicals (Fig. 2). The trapping of carbon-centered radicals eliminates the paramagnetism of the nitroxide moiety and inhibits the intramolecular quenching. The results demonstrate that **1** can be used as an off/on luminescence probe for carbon-centered radicals. A control experiment was performed by using a solution of **1** without AIBN, and no obvious enhancement of Tb luminescence was observed (Fig. 2). Concomitant with the increase in Tb luminescence was a decrease in EPR signal of TEMPO moiety as expected (Fig. S2†). Both luminescence and EPR signal responsive to the radical trapping process make the spin-labeled lanthanide complex **1** a potential bimodal probe. As the spin-labeled luminescent probes for carbon-centered radicals are finding increased use in a wide range of applications, this spin-labeled lanthanide complex, with its lanthanide-luminescence properties, would be a promising tool in analytical chemistry and photochemistry.

### Response of **1** to hydroxyl radicals

The hydroxyl radical (OH) is one of the most powerful oxidative reactants of the reactive oxygen species (ROS).<sup>39</sup> The application of spin-labeled fluorescent probes for the detection of hydroxyl radicals is based on the reaction of OH with DMSO to produce quantitatively a methyl radical ( $\text{CH}_3$ ),<sup>48</sup> which was then trapped by the nitroxide moiety of **1**, for the nitroxide radical does not trap the hydroxyl radical directly. In this present work, the response of **1** to hydroxyl radicals was explored. The hydroxyl radicals were generated *via* photolysis of nitrate ions ( $\text{NO}_3^-$ ),<sup>49</sup> and this method is easily manipulated through irradiation time setting. With sufficient  $\text{KNO}_3$  and DMSO, the amount of OH produced was proportional to the irradiation time, and thus proportional to the amount of  $\text{CH}_3$ . As shown in Fig. 3, the intensity of Tb luminescence increased linearly with irradiation

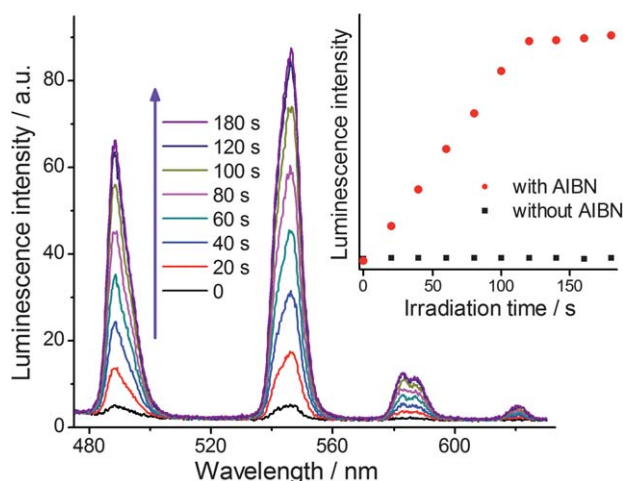


**Fig. 2** Tb luminescence spectra of **1** ( $\lambda_{\text{ex}} = 340 \text{ nm}$ ) and Tb luminescence enhancement ( $\lambda_{\text{em}} = 546 \text{ nm}$ , inset, a control experiment also presented), resulted from carbon-centered radical-trapping, as a function of irradiation time. The concentrations of **1** and AIBN were  $2 \mu\text{M}$  and  $1 \text{ mM}$ , respectively, irradiated with UV light ( $\lambda > 350 \text{ nm}$ ). The solution was  $10 \text{ mM}$  Tris-HCl buffer at pH 7.4, containing 10% methanol.



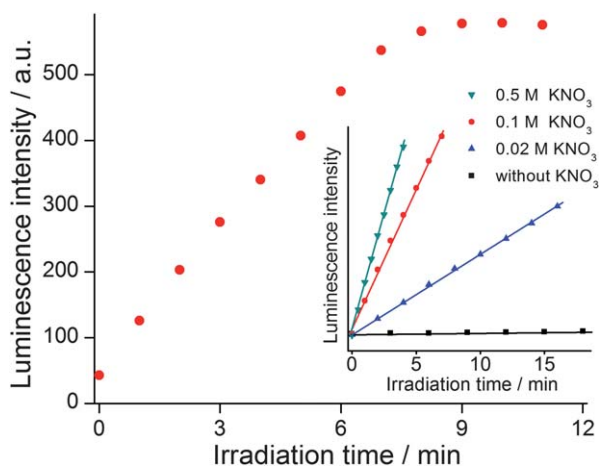


**Fig. 3** Tb luminescence enhancement ( $\lambda_{\text{ex}} = 340$  nm,  $\lambda_{\text{em}} = 546$  nm) of the solution of **1** as a function of irradiation time of  $\text{KNO}_3$  photolysis. There were  $2 \mu\text{M}$  **1**,  $0.1$  M  $\text{KNO}_3$  and  $1$  M DMSO in  $10$  mM Tris-HCl buffer at pH  $7.4$ , irradiated with UV light ( $\lambda > 300$  nm). (inset) The influence of  $\text{KNO}_3$  concentration on the rate of Tb luminescence enhancement. The experimental conditions were unchanged, except the concentration of  $\text{KNO}_3$ .

time at first, attributable to the production of complex **4** (Chart 1); and then leveled off after a period of time, attributable to the completely transformation of **1** to **4**. The rate of  $\text{OH}$  generation varied according to the concentration of  $\text{KNO}_3$ , and a  $\text{KNO}_3$ -free solution showed no significant increase of Tb luminescence (Fig. 3 inset). In the linear responsive range, the concentration of **4** was calibrated by comparing the luminescence increment with the overall increment when the luminescence reached a maximum. And the concentration of  $\text{OH}$  was calibrated by assuming that one  $\text{OH}$  molecule produced one molecule of **4** in this model experiment. Defining the detection limit as the concentration corresponding to three standard deviations of the background signal, we estimated a detection limit of  $4$  nM for  $\text{OH}$ . The result demonstrates that this spin-labeled lanthanide-based probe **1** can be used as a sensitive probe for  $\text{OH}$ .

As a lanthanide-based probe, the long luminescence lifetime makes the time resolved measurement feasible. To demonstrate the utility of the long lifetime of lanthanide luminescence, we contrasted the time-resolved spectra with steady-state spectra of **1** in the measurement of  $\text{OH}$ . With a gated detection, the long-lived Tb luminescence of diamagnetic compound **4** can be distinguished from the short-lived fluorescence and scattered light (Fig. 4). The long luminescence lifetime endows this probe with great potential in time-resolved luminescence microscopy.

### The quenching process of lanthanide luminescence

As mentioned above, the sensitised lanthanide luminescence generally undergoes three excited states after the sensitizer is excited. The absorption spectra did not show obvious difference between **1** and **2** (Fig. S3†), indicating that the nitroxide radical does not affect the absorption transition of the cs124 moiety.

The luminescence intensity of cs124 moiety (centered at  $367$  nm) in **1** was about  $2.3$  times weaker than that of its diamagnetic analogue **2** (Fig. 1). The cs124 luminescence of **1**

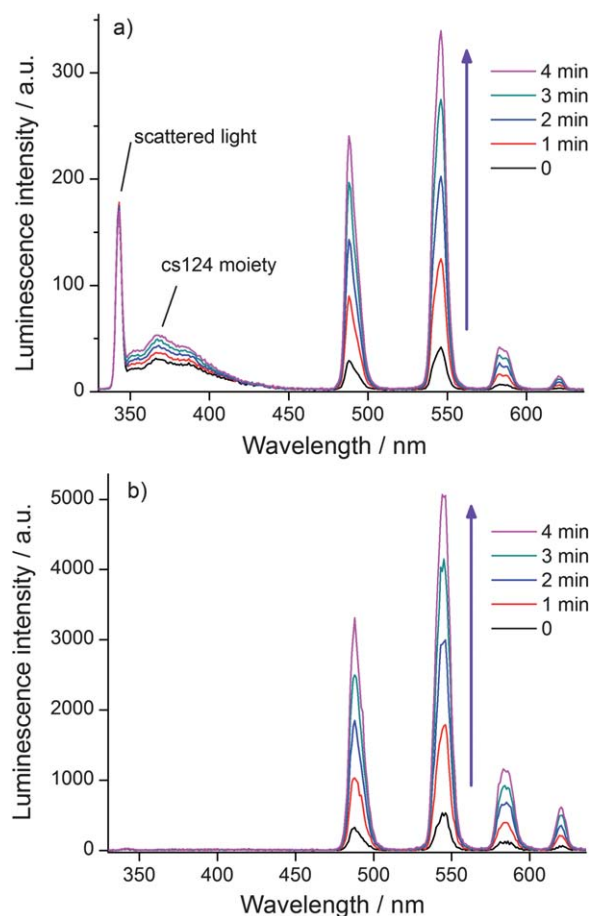


**Fig. 4** (a) The steady-state spectra ( $\lambda_{\text{ex}} = 340$  nm) and (b) the time-resolved spectra ( $\lambda_{\text{ex}} = 340$  nm, delay time =  $0.3$  ms and gate time =  $3$  ms) of the solution of **1** as a function of irradiation time of  $\text{KNO}_3$  photolysis. The experimental conditions were the same as in Fig. 3.

decayed more quickly than that of **2** (Fig. 5), and the decrease extent in cs124 singlet excited state lifetime resulted from nitroxide quenching is nearly equal to that of its fluorescence intensity quenching. The intramolecular quenching of the singlet

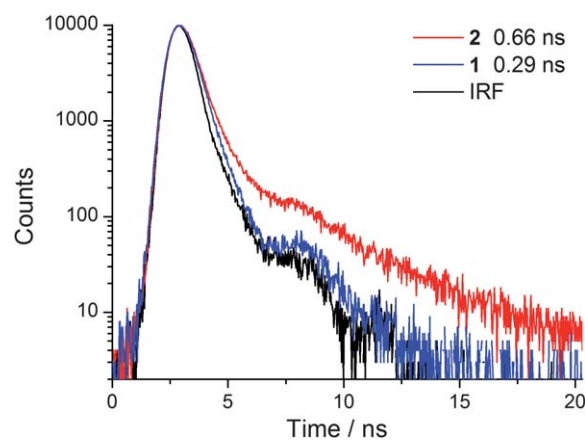


**Fig. 5** Fluorescence decays of cs124 moiety ( $\lambda_{\text{ex}} = 281$  nm) of **1** and **2**. The photons were collected at the wavelength of  $367$  nm; the instrument response function (IRF) was also presented.

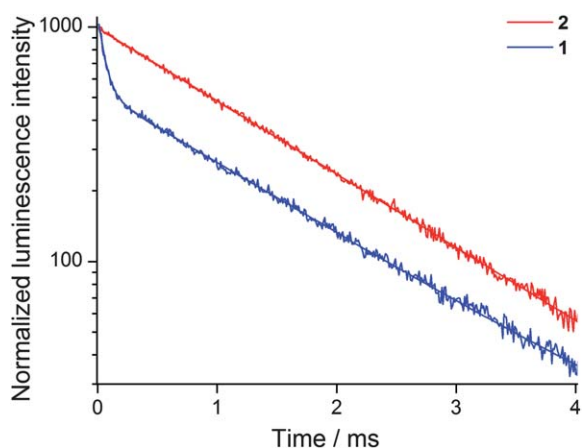


Fig. 6 Tb luminescence decays ( $\lambda_{\text{ex}} = 340 \text{ nm}$ ,  $\lambda_{\text{em}} = 546 \text{ nm}$ ) of **1** and **2**.

excited states of various organic fluorophores by nitroxide has been studied extensively. The quenching efficiency has been proved to be related to the distance and orientation of the nitroxide with respect to the fluorophore,<sup>21,22</sup> and quenching efficiencies from 2-fold to several 100-fold have been observed.<sup>21,22,24</sup>

The Tb luminescence decay of **2** was well fitted with single exponential decay, and had a lifetime of 1.40 ms (Fig. 6), a typical long lifetime of the lanthanide complex. The Tb luminescence decay of **1** was well fitted with a bi-exponential decay (Fig. 6). The shorter-lived component (0.06 ms) was attributed to **1** itself. The much shorter lifetime implicated that the nitroxide quenched the Tb excited state efficiently. A previous paper also reported that the luminescence of Tb<sup>3+</sup>/EDTA was quenched by 4-hydroxy-TEMPO intermolecularly,<sup>23</sup> where the excited state of terbium was directly quenched by the nitroxide radical for there was no sensitiser present. The lifetime of the longer-lived component (1.42 ms) agreed closely with that of **2**, suggesting the presence of a small percentage of highly luminescent Tb complex without nitroxide radical labeled.

## Conclusions

Herein we report the design and synthesis of a spin-labeled terbium-based bimodal probe, Tb<sup>3+</sup>/cs124-DTPA-TEMPO, for free radicals. The lanthanide complex probe shows a large EPR signal resulting from the nitroxide radical moiety and is weakly luminescent resulting from the intramolecularly quenching effect of the nitroxide radical on sensitised terbium luminescence. The intensities of both EPR and luminescence can be modulated by eliminating the paramagnetism of the nitroxide moiety through trapping a carbon-centered radical analyte and thus give a quantification of the analyte. In the probe, the nitroxide radical acts as a switch to the Tb luminescence, and a trapper of carbon-centered radical as well. The study of the quenching process has demonstrated that the nitroxide moiety quenches multiple excited states of the lanthanide complex. These results would certainly facilitate a deeper understanding of nitroxide radical quenching theory. As a preliminary study of application, the response of this probe toward model carbon-centered radicals and hydroxyl radicals has been explored. A detection limit of

4 nM for OH was obtained. The preparation of the probe is straightforward, and it is water-soluble and favorable for a time-resolved luminescence technique. These advantages make it a promising sensor to monitor free radical processes in various areas of photochemistry and biochemistry. This probe is the first example of spin-labeled lanthanide complexes, which might initiate a new field beyond the conventional spin-labeled organic fluorophore probes and expands the application of lanthanide complexes.

## Acknowledgements

This work was supported by the National Natural Science Foundation of China (20375032, 20675068, 20835005, 20975086).

## Notes and references

- C. P. Montgomery, B. S. Murray, E. J. New, R. Pal and D. Parker, *Acc. Chem. Res.*, 2009, **42**, 925–937.
- J. C. G. Bünzli, *Chem. Rev.*, 2010, **110**, 2729–2755.
- J. L. Yuan and G. L. Wang, *Trends Anal. Chem.*, 2006, **25**, 490–500.
- A. Thibon and V. C. Pierre, *Anal. Bioanal. Chem.*, 2009, **394**, 107–120.
- T. Terai, K. Kikuchi, S. Y. Iwasawa, T. Kawabe, Y. Hirata, Y. Urano and T. Nagano, *J. Am. Chem. Soc.*, 2006, **128**, 6938–6946.
- B. Song, G. L. Wang and J. L. Yuan, *Chem. Commun.*, 2005, 3553–3555.
- B. Song, G. L. Wang, M. Q. Tan and J. L. Yuan, *J. Am. Chem. Soc.*, 2006, **128**, 13442–13450.
- R. A. Poole, F. Kielar, S. L. Richardson, P. A. Stenson and D. Parker, *Chem. Commun.*, 2006, 4084–4086.
- See <http://www.htrf.com/>.
- M. K. Johansson, R. M. Cook, J. D. Xu and K. N. Raymond, *J. Am. Chem. Soc.*, 2004, **126**, 16451–16455.
- M. Togashi, Y. Urano, H. Kojima, T. Terai, K. Hanaoka, K. Igarashi, Y. Hirata and T. Nagano, *Org. Lett.*, 2010, **12**, 1704–1707.
- K. Hanaoka, K. Kikuchi, H. Kojima, Y. Urano and T. Nagano, *J. Am. Chem. Soc.*, 2004, **126**, 12470–12476.
- M. Halim, M. S. Tremblay, S. Jockusch, N. J. Turro and D. Sames, *J. Am. Chem. Soc.*, 2007, **129**, 7704–7705.
- S. Mizukami, K. Tonai, M. Kaneko and K. Kikuchi, *J. Am. Chem. Soc.*, 2008, **130**, 14376–14377.
- U. Karhunen, L. Jaakkola, Q. Wang, U. Lamminmäki and T. Soukka, *Anal. Chem.*, 2010, **82**, 751–754.
- A. Thibon and V. C. Pierre, *J. Am. Chem. Soc.*, 2009, **131**, 434–435.
- Y. Kitamura, T. Ihara, Y. Tsujimura, Y. Osawa, M. Tazaki and A. Jyo, *Anal. Biochem.*, 2006, **359**, 259–261.
- A. Potapov, H. Yagi, T. Huber, S. Jergic, N. E. Dixon, G. Otting and D. Goldfarb, *J. Am. Chem. Soc.*, 2010, **132**, 9040–9048.
- N. Barhate, P. Cekan, A. P. Massey and S. T. Sigurdsson, *Angew. Chem., Int. Ed.*, 2007, **46**, 2655–2658.
- G. I. Likhtenstein, K. Ishii and S. Nakatsuji, *Photochem. Photobiol.*, 2007, **83**, 871–881.
- S. Green and M. A. Fox, *J. Phys. Chem.*, 1995, **99**, 14752–14757.
- S. A. Green, D. J. Simpson, G. Zhou, P. S. Ho and N. V. Blough, *J. Am. Chem. Soc.*, 1990, **112**, 7337–7346.
- J. Matko, K. Ohki and M. Edidin, *Biochemistry*, 1992, **31**, 703–711.
- S. E. Herbelin and N. V. Blough, *J. Phys. Chem. B*, 1998, **102**, 8170–8176.
- K. E. Fairfull-Smith, J. P. Blinco, D. J. Keddie, G. A. George and S. E. Bottle, *Macromolecules*, 2008, **41**, 1577–1580.
- C. Coenjarts, O. Garcia, L. Llauger, J. Palfreyman, A. L. Vinette and J. C. Scaiano, *J. Am. Chem. Soc.*, 2003, **125**, 620–621.
- A. Aspée, O. Garcia, L. Marette, R. Sastre and J. C. Scaiano, *Macromolecules*, 2003, **36**, 3550–3556.
- A. S. Micallef, J. P. Blinco, G. A. George, D. A. Reid, E. Rizzardo, S. H. Thang and S. E. Bottle, *Polym. Degrad. Stab.*, 2005, **89**, 427–435.
- M. G. Ivan and J. C. Scaiano, *Photochem. Photobiol.*, 2003, **78**, 416–419.

- 30 Y. M. Dang and X. Q. Guo, *Appl. Spectrosc.*, 2006, **60**, 203–207.
- 31 M. Jia, Y. Tang, Y. F. Lam, S. A. Green and N. V. Blough, *Anal. Chem.*, 2009, **81**, 8033–8040.
- 32 N. V. Blough and D. J. Simpson, *J. Am. Chem. Soc.*, 1988, **110**, 1915–1917.
- 33 B. Miljevic, K. E. Fairfull-Smith, S. E. Bottle and Z. D. Ristovski, *Atmos. Environ.*, 2010, **44**, 2224–2230.
- 34 T. M. Flicker and S. A. Green, *Environ. Health Perspect.*, 2001, **109**, 765–771.
- 35 B. Miljevic, M. F. Heringa, A. Keller, N. K. Meyer, J. Good, A. Lauber, P. F. Decarlo, K. E. Fairfull-Smith, T. Nussbaumer, H. Burtcher, A. S. H. Prevot, U. Baltensperger, S. E. Bottle and Z. D. Ristovski, *Environ. Sci. Technol.*, 2010, **44**, 6601–6607.
- 36 B. B. Li, P. L. Gutierrez and N. V. Blough, *Anal. Chem.*, 1997, **69**, 4295–4302.
- 37 X. F. Yang and X. Q. Guo, *Analyst*, 2001, **126**, 1800–1804.
- 38 B. B. Li, N. V. Blough and P. L. Gutierrez, *Free Radical Biol. Med.*, 2000, **29**, 548–556.
- 39 P. P. Vaughan and N. V. Blough, *Environ. Sci. Technol.*, 1998, **32**, 2947–2953.
- 40 Q. Zhu, Y. X. Lian, S. Thyagarajan, S. E. Rokita, K. D. Karlin and N. V. Blough, *J. Am. Chem. Soc.*, 2008, **130**, 6304–6305.
- 41 M. Alaghmand and N. V. Blough, *Environ. Sci. Technol.*, 2007, **41**, 2364–2370.
- 42 S. A. Rivera and B. S. Hudson, *J. Am. Chem. Soc.*, 2006, **128**, 18–19.
- 43 M. Li and P. R. Selvin, *J. Am. Chem. Soc.*, 1995, **117**, 8132–8138.
- 44 S. R. Meech and D. Phillips, *J. Photochem.*, 1983, **23**, 193–217.
- 45 P. H. Ge and P. R. Selvin, *Bioconjugate Chem.*, 2004, **15**, 1088–1094.
- 46 W. R. Couet, R. C. Brasch, G. Sosnovsky, J. Lukszo, I. Prakash, C. T. Gnewuch and T. N. Tozer, *Tetrahedron*, 1985, **41**, 1165–1172.
- 47 V. Maurel, M. Laferrière, P. Billone, R. Godin and J. C. Scaiano, *J. Phys. Chem. B*, 2006, **110**, 16353–16358.
- 48 M. K. Eberhardt and R. Colina, *J. Org. Chem.*, 1988, **53**, 1071–1074.
- 49 R. G. Zepp, J. Holgné and H. Bader, *Environ. Sci. Technol.*, 1987, **21**, 443–450.